

Mechanism of Gas Phase Ethene-Ozone Reaction and Concomitant Processes. Theoretical Study

Robert Ponec,^{a,*} Jana Roithová,^a and Yehuda Haas^b

^a *Institute of Chemical Process Fundamentals, Czech Academy of Sciences, Prague 6, Suchbát, 165 02, Czech Republic*

^b *Department of Physical Chemistry and the Farkas Center for Light Induced Processes, The Hebrew University of Jerusalem, 91904, Jerusalem, Israel*

Received April 12, 2000; revised July 24, 2000; accepted October 20, 2000

A theoretical analysis of the gas phase ethene-ozone reaction is presented. A complete survey of low energy channels reveals several new intermediates, and provides a rationale for the efficient formation of OH radicals in the gas phase ozonolysis of ethene.

Key words: ethene-ozone reaction, ozonolysis of ethene, reaction channels.

INTRODUCTION

Since its discovery in 1855,¹ the reaction of unsaturated organic molecules with ozone, the so-called ozonolysis, has attracted attention of organic chemistry not only for its broad synthetic potential^{2–6} but also for its possible use as an analytical tool in structure elucidations. In addition to these well-known and thoroughly reviewed applications, interest in the study of ozonolysis has been revived in recent years mainly due to its ecological importance. In this respect, attention is increasingly being paid to the study of gas phase ozone-alkene reactions, which play a crucial role in various processes in atmospheric chemistry^{7–10} such as, for example, in the photochemical smog production¹¹ and as a source of organic acids and hydroperoxides in the troposphere.^{12–14} The scope of these studies is very broad and ranges

* Author to whom correspondence should be addressed.

from purely experimental investigations of the kinetics and the mechanism of alkene-ozone reaction¹⁵⁻²⁶ to theoretical reports aiming at a detailed microscopic insight into the individual reaction steps of the basic Criegee mechanism²⁷ as well as of the concomitant processes.²⁸⁻³⁹

The nowadays generally accepted Criegee mechanism²⁷ assumes that the ozonolysis proceeds in three basic steps:

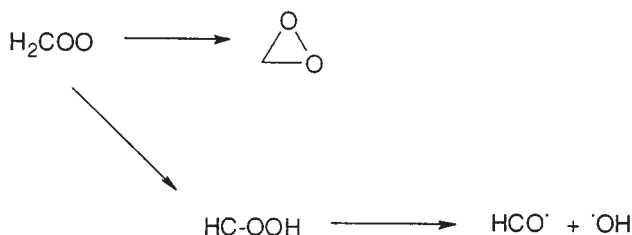
- i) formation of 1,2,3-trioxolane (the so-called primary ozonide, POZ) in the first, 1,3-dipolar cycloaddition step of ozone to the alkene double bond.
- ii) splitting of the primary ozonide into a mixture of carbonyl component (CC) and reactive carbonyl oxide (COX), often called Criegee intermediate.
- iii) the retro-cycloaddition of CC and COX to form the final or secondary ozonide (SOZ).

This mechanism is, however, predominantly operative in solution, where due to efficient dissipation of excess energy, the reaction follows the minimum energy Criegee path and secondary ozonides can often be isolated in high yields.

The situation with the gas phase reaction is, however, slightly different, since many of the transient species generated by primary splitting of POZ have enough excess energy to overcome the energy barriers, opening new reaction channels for their decay. To take these concomitant processes into account, the original Criegee mechanism was modified. Such a modification usually assumes that the main precursor of these processes is the energy-rich molecule of COX formed by the splitting of the primary ozonide.

An example of such a modified mechanism was recently analyzed by Cremer and coworkers,³⁹ who considered that the main side-reaction of energy-rich COX was its rearrangement to the isomeric dioxirane and hydroperoxycarbene (Scheme 1).

The main problem of the theoretical description of the above reaction scheme is that, because of the biradicaloid nature of ozone, carbonyl oxide



Scheme 1

and some other participating species, calculations of extremely high quality are required and a satisfactory inclusion of electron correlation is absolutely necessary. The best so far reported calculations involving the complete Criegee mechanism were recently performed using the density functional theory at B3LYP/6-31G** level, but even this sophisticated approach failed to properly describe even the first step of the reaction.³⁵ Sufficient reliability of the calculations can be reached, as shown by Olzman,³⁵ only at the CCSD(T)/TZ+2P level of theory. Calculations of such sophistication can even now be performed only for systems with three heavy atoms, so that even for the simplest case of parent ethene-ozone reaction only some reaction steps, but not the whole reaction scheme, could be analyzed. We can thus see that, despite appreciable progress in computation methodology, reliable theoretical analysis of the whole ozonolysis mechanism is still beyond the reach of even the contemporary state-of-the-art calculations. As a consequence, our knowledge of the mechanism of ozonolysis is still far from complete and, except for the above mentioned study by Olzman,³⁵ there are very scarce reliable data about the individual processes participating in the mechanism of ozonolysis.

In an attempt to obtain a consistent picture of the whole gas-phase reaction mechanism, we decided to perform a detailed study of the potential energy surface of the reacting $C_2H_4O_3$ system at a lower, but completely consistent semi-empirical AM1 level of theory. We are, of course, aware of the simplicity of such an approach in the light of present standards, but since the other feasible alternative applicable to a thorough potential energy scan, the *ab-initio* SCF calculations with MP2 correlation correction, was shown to be insufficiently satisfactory,³⁹ we assume that at this point a complete semi-empirical study of this system can provide a valuable insight into the gas-phase mechanism. This method cannot be trusted to provide correct *absolute* values of energy barriers for individual reaction steps, but we believe that the trends revealed by the *relative* energies calculated for individual steps represent the physical reality.

RESULTS AND DISCUSSION

The main goal of our analysis of gas-phase ozone-alkene reaction was to perform a thorough potential energy scan of the $C_2H_4O_3$ reactive system. Being aware of the necessity to include electron correlation in describing the species participating in this reaction, we first performed the potential energy scan using *ab-initio* SCF calculations in 6-31G** basis with MP2 correction for correlation. The calculations were performed using the PC Gamess version⁴⁰ of the Gamess-US QC package.⁴¹ Some calculated results for the

TABLE I

Ab-initio calculated values of energies and enthalpies of the species participating in the Criegee mechanism of ozonolysis^a

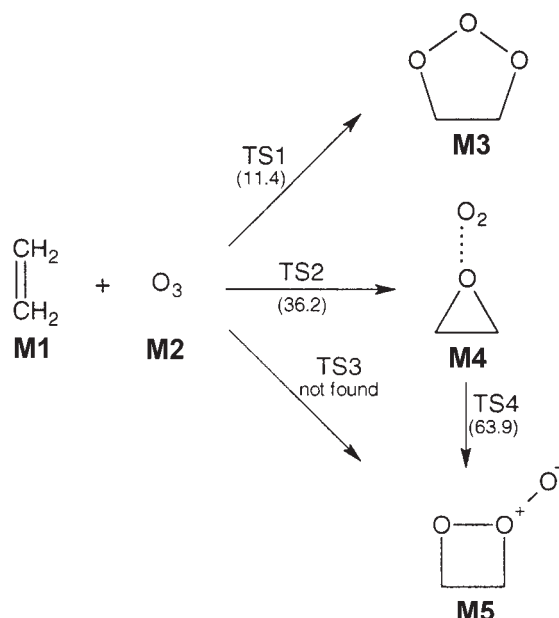
system	abbrev.	RHF		MP2				
		E_0 kcal mol ⁻¹	E_0 kcal mol ⁻¹	ZPE kcal mol ⁻¹	H kcal mol ⁻¹	E_0 +ZPE kcal mol ⁻¹	E_0 +H kcal mol ⁻¹	
ethene	M1	-48970.37	-49145.07	32.79	35.29	-49112.28	-49109.78	
ozone	M2	-140726.96	-141108.55	6.11	8.56	-141102.44	-141099.99	
	TS1	-189683.27	-190250.10	39.68	43.26	-190210.42	-190206.84	
primary ozonide	M3	-189783.42	-190302.31	42.58	45.99	-190259.73	-190256.32	
	TS5	-189729.64	-190289.32	39.88	43.68	-190249.44	-190245.64	
formaldehyde	M6	-71454.73	-71651.64	17.22	19.61	-71634.42	-71632.03	
carbonyl oxide	M7	-118325.43	-118636.74	19.67	22.33	-118617.07	-118614.41	
dipole complex	M10	-189788.50	-190297.17	39.53	44.08	-190257.64	-190253.09	
	TS9	-189781.59	-190296.98	40.01	43.86	-190256.97	-190253.12	
secondary ozonide	M11	-190348.50	-190352.14	43.76	47.02	-190308.38	-190305.12	

^a Calculations were performed using PC-Gamess program version⁴⁰ of the Gamess-US QC package⁴¹ in 6-31G** basis.

species participating in the basic Criegee mechanism are summarized in Table I. In keeping with previous findings by the Cremer group,³⁹ this level of theory is clearly not capable of giving a reliable description of the process. For example, the MP2 calculated barrier for the first cycloaddition step leading to the POZ is negative, while the experimental value is around 5 kcal mol⁻¹.¹⁵ Similarly dubious results were calculated also for other reaction steps. Using a simple semi-empirical approach, we performed a scan of the complete potential energy surface. This scan revealed the minima and transition states for the species participating in the basic Criegee mechanism but, in addition, the minima and transition states at relatively low energies were found for other concomitant processes. A complete list of the energetic data is summarized in Table II. The results of this scan reveal a complex reaction scheme, which may be represented by five distinct steps. In the following part, we discuss each of these steps separately.

Step 1

The ozonolysis reaction is initiated by the attack of ozone on the alkene double bond, leading to the formation of an unstable intermediate, the so-called molozonide. Although there was some discussion concerning the



Scheme 2. The values in parentheses (kcal mol⁻¹) refer to the activation barriers of individual reaction steps.

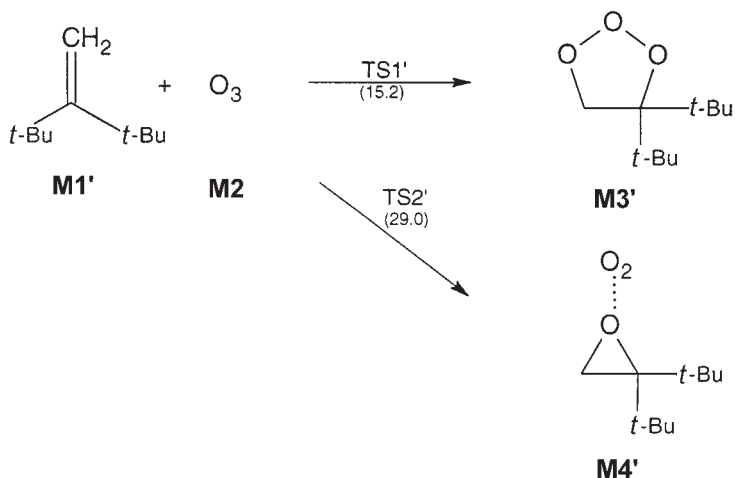
TABLE II

AM1 calculated heats of formation of the species localized as minima or transition states on the PE surface of the reactive $C_2H_4O_3$ system

system	abbrev.	method	$\frac{\Delta H}{\text{kcal mol}^{-1}}$	system	abbrev.	method	$\frac{\Delta H}{\text{kcal mol}^{-1}}$
ethene	M1	RHF	16.5		TS12	RHF	65.0
ozone	M2	RHF	37.8		TS13	RHF	86.5
	TS1	RHF	65.7	hydroperoxy carbene	M14	RHF	48.1
primary ozonide	M3	RHF	5.6		TS14	RHF	57.2
	TS2	RHF	90.5		B2	UHF	-2.0
complex oxirane-oxygen	M4	RHF	-10.0		B3	UHF	0.6
	TS3		not found		TS15		22.1
	TS4	RHF	53.9		B4	UHF	-34.8
isoozonide	M5	RHF	48.8		TS16	UHF	-1.7
	TS5	RHF	25.1		TS17	UHF	not found
formaldehyde	M6	RHF	-31.5		B5	UHF	-10.7
carbonyl oxide	M7	RHF	30.7		TS18	RHF	26.5
	TS6	RHF	53.6	formic acid	M15	RHF	-97.4
acetaldehyde	M8	RHF	-41.6		TS19	RHF	18.8
oxygen	M9	RHF	0.7	3-hydroxydioxetane	M16	RHF	-37.8
	TS7	UHF	19.6		TS20	RHF	3.1
	TS8	RHF	53.6		TS21	RHF	not found
dipole complex	B1	UHF	-13.1		B6	UHF	-65.6
	M10	RHF	-5.3		TS22	UHF	-28.6
	TS9	RHF	-3.0		TS23	UHF	-27.2
secondary ozonide	M11	RHF	-63.5		TS24	RHF	-7.5
	TS10	RHF	28.6	hydroxymethylformiate	M17	RHF	-146.3
dioxirane	M12	RHF	22.3		TS25	RHF	-101.9
	TS11	RHF	32.6		TS26	RHF	-3.0
hydroperoxyacetaldehyde	M13	RHF	-61.0				

structure of this molozonide⁴² and, for example, in early years the structure **M5** was proposed by Staudinger,⁴³ the nowadays preferred one is the structure **M3**, based on Criegee's proposal, who identified the molozonide with the 1,2,3-trioxolane, now often called primary ozonide (POZ). This structure has been experimentally observed by microwave spectroscopy⁴⁴ and is now the accepted one.

In our potential-energy scan, we were able to localize both POZ and the structure **M5** as minima on the potential energy surface and also the transition state TS1 leading from the initial reactants to POZ. The attempts to localize also the other transition state TS3 for the formation of **M5** were, however, unsuccessful. Despite that, it is possible to expect that, owing to a much higher energy content of the structure **M5** compared to POZ, also the energy barrier leading to its formation will be substantially higher. The formation of POZ can thus be regarded as the energetically most favorable path of initiating the ozonolysis. This conclusion remains valid even if another reaction path leading to the formation of oxirane...oxygen complex is localized together with the corresponding transition state TS2. Although the corresponding energy barrier is apparently too high to allow a substantial population of this reaction channel in this particular case, the formation of oxiranes has indeed been reported in the ozonolysis of sterically hindered alkenes.^{45,46} Consistent with this observation, we have been able to show that the ratio of the activation energies for the basic Criegee path and the formation of oxiranes does indeed decrease on going from ethene to the sterically crowded 1,1-di-*tert*-butylethene (Scheme 3).

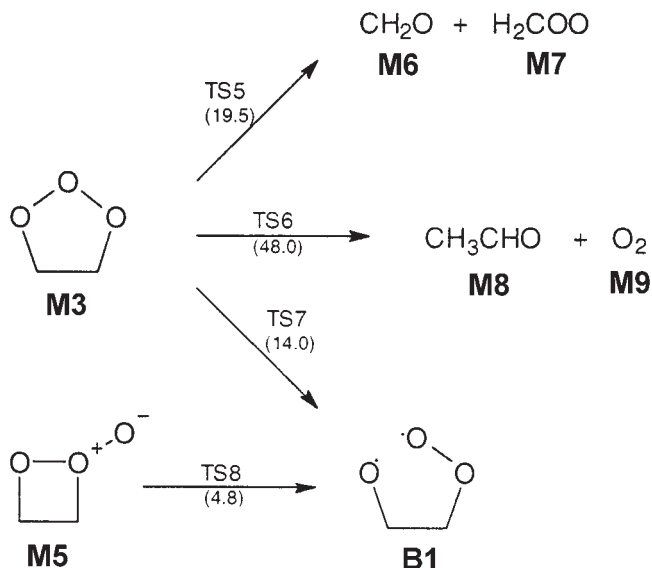


Scheme 3. The values in parentheses (kcal mol⁻¹) refer to the activation barriers of individual reaction steps.

Step 2

Based on the results of the PE scan, the second step of the reaction mechanism consists of reaction channels leading to unimolecular decay of the primarily formed POZ. According to the basic Criegee mechanism, such decay proceeds *via* the concerted splitting of POZ (TS5), forming the CC and COX pair. Clearly, this reaction path is electronically favorable also according to our PE scan but, in addition, we have been able to elucidate also some other reaction paths.

One of them, corresponding to the primary splitting of O-O bond in POZ and leading to biradical intermediate **B1** is energetically even less demanding, as compared to the classical Criegee path, and certainly cannot be excluded as an alternative to the concerted path. This result is very interesting since, based on earlier thermochemical studies by Benson,⁴⁷ the non-concerted path of the splitting of POZ was usually excluded from the considerations. As it can be seen from Scheme 4, the non-concerted and the concerted paths are energy-comparable, even if we admit that stability of the open-shell transition state (TS7) and the corresponding intermediate **B1** can be slightly exaggerated in our calculations due to the systematic bias of the UHF approach used. Participation of this non-concerted reaction path is important, especially because the rearrangement of the resulting biradical

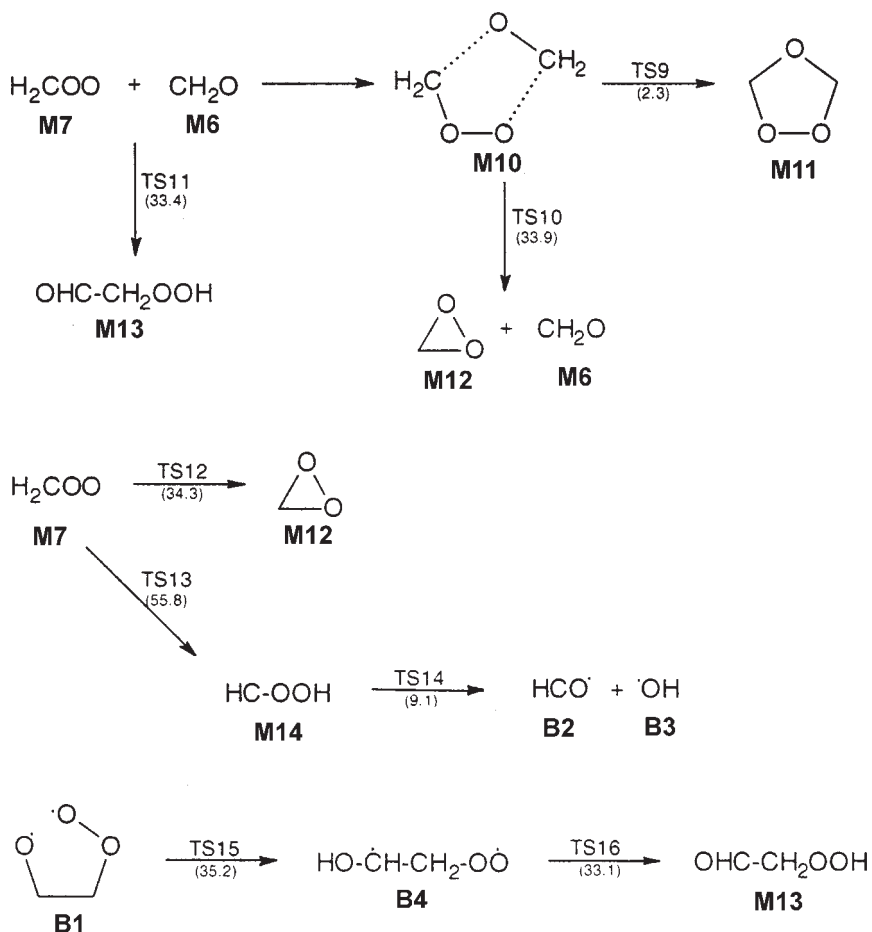


Scheme 4. The values in parentheses (kcal mol^{-1}) refer to the activation barriers of individual reaction steps.

intermediate **B1**, taking place in further steps, opens a new efficient channel for the formation of hydroperoxides, which serve as the main precursors of OH radicals in the troposphere. It is interesting to note that the biradical **B1** can be also formed by cleavage of Staudinger's molozonide **M5**.

Step 3

This step describes the destiny of COX and other transient species formed by the splitting of POZ. As it can be seen from Scheme 5, the most energetically favorable of all these processes is the classical Criegee paths



Scheme 5. The values in parentheses (kcal mol^{-1}) refer to the activation barriers of individual reaction steps.

leading, *via* the postulated dipole complex DC (**M10**),^{33,34} to the formation of 1,2,4-trioxolane, the so-called SOZ (**M11**).

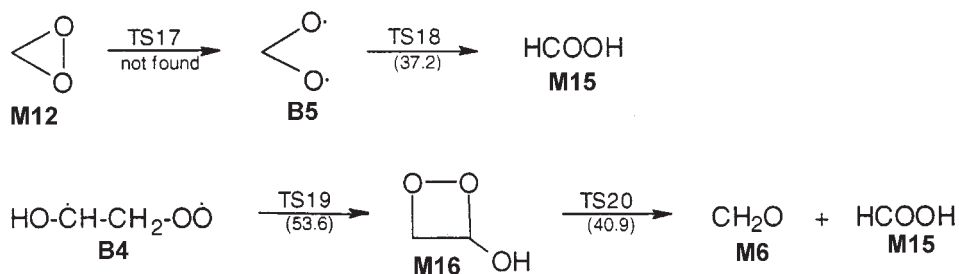
This path is usually preferred in solution ozonolysis, where the efficient dissipation of excess energy allows the system to follow the least energy path but, as reported in a recent IR-laser study,⁴⁸ secondary ozonides can be formed in high yields also in a low temperature gas-phase ethene-ozone reaction.

At ordinary temperatures, however, the classical Criegee path is accompanied by several reactions, which, although energetically more demanding, still represent plausible and efficient reaction channels for the decay of energy-rich species formed by the splitting of POZ. Some of these paths, describing the destiny of the reactive COX, were recently studied by Cremer's group,^{37,39} and their data can be used as a certain standard with which our AM1 results can be confronted. Thus, *e.g.*, Cremer reports the rearrangement of COX to dioxirane (**M12**) to be roughly 13 kcal mol⁻¹ more favorable than its alternative transformation to hydroperoxycarbene (**M14**), which might serve as a precursor for the formation of OH radicals. Quite in keeping with this observation are also the results of our AM1 analysis.

As can be seen from Scheme 5, the rearrangement of COX to dioxirane is clearly more favorable than an alternative path to hydroperoxycarbene (**M14**). In addition to qualitatively reproducing previous results of Cremer, we report here that there are also some other reaction channels, not considered so far, whose evaluation would certainly be desirable so as to make the picture of the mechanism of the gas phase ozonolysis more realistic. Among such new reaction channels, it is worthwhile mentioning, for example, the direct isomerization of the dipole complex **M10** to dioxirane and formaldehyde *via* the TS10, the rearrangement of COX and CC to hydroperoxy-acetaldehyde OCHCH₂OOH (**M13**), and the transformation of biradical intermediate **B1** to the isomeric biradical HO-CH-CH₂OOH (**B4**). This biradical subsequently transforms to the hydroperoxy-acetaldehyde OCHCH₂OOH (**M13**), which serves as the precursor for the production of OH radicals in subsequent steps.

Step 4

This step involves the decomposition pathways of dioxirane to formic acid *via* **B5** as well as the concomitant transformations of the biradical intermediate **B4** (Scheme 6). None of these reactions has been studied so far by either *ab-initio* or semiempirical methods, so the reported results (Table II) represent the first theoretical data for these processes. In the PE scan for the decomposition of dioxirane, the biradical structure **B5**, usually assumed to be the intermediate in the isomerization to HCOOH, was indeed localized



Scheme 6. The values in parentheses (kcal mol⁻¹) refer to the activation barriers of individual reaction steps.

as a minimum on the PE hypersurface, but unfortunately the attempts to localize also the corresponding transition state (TS17) were not successful. As it can be seen from Table II, and quite in keeping with the Hammond postulate, the barrier can be expected to be fairly low. We have, however, localized the transition state (TS18) for the isomerization of **B5** to formic acid.

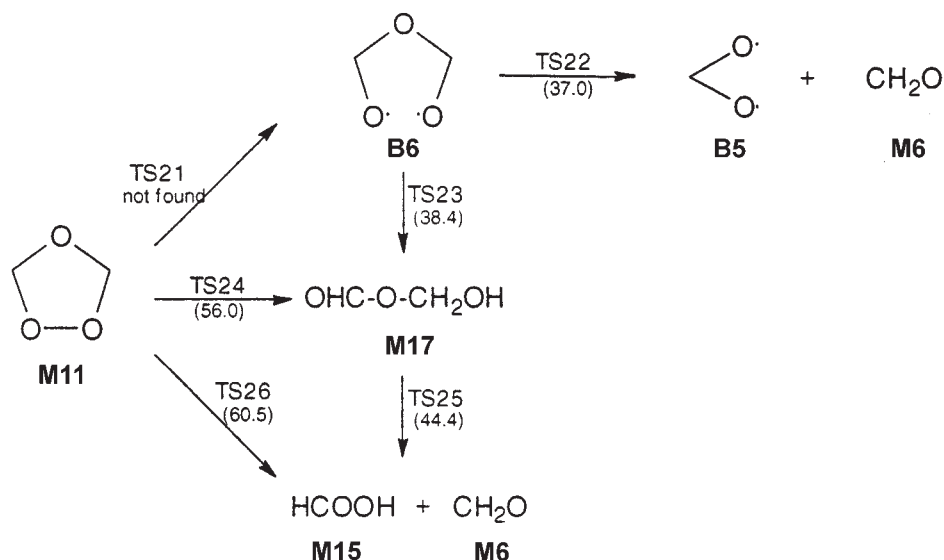
In contrast to incomplete localization of critical points for the isomerization of dioxirane, the potential energy scan for the decay of biradical **B4** was completely successful and all the species participating in the corresponding reaction path were localized as minima or transition states on the PE hypersurface. An interesting feature of this hypersurface is the presence of the **M16** species, which opens a new feasible path for the formation of HCOOH and CH₂O.

Step 5

The final step of our PE scan concerned the decomposition pathways of the secondary ozonide SOZ. Like in the previous case, this process did not receive any systematic attention either and the only reported theoretical study was published by Dewar²⁸ using the semi-empirical AM1 approach. In his study, Dewar assumes two possible pathways for the decomposition of SOZ; the stepwise process *via* the biradical intermediate (presumably **B6**), and the concerted process *via* the transition state TS26. Although no numerical data were reported for the stepwise path, Dewar claims that the concerted path is more favorable.

Because of the lack of data for the stepwise non-concerted path, we performed a detailed PE scan in which an open-shell biradical **B6**, identical to the biradical presumed by Dewar²⁸ was localized as a minimum on the PE hypersurface. In addition to this biradical, also the transition states for its isomerization to **B5** + CH₂O (TS22) as well as for the direct rearrangement to hydroxymethylformate (TS 23) were localized.

Unfortunately, the attempts to localize also the TS21 for the formation of **B6** from SOZ failed. We believe, however, that the barrier to this process, which involves only the splitting of the relatively weak O-O bond, will not be very high. In addition to the above stepwise reaction channels, we have been able to localize also the transition states TS24 and TS26 for the concerted rearrangement of SOZ to hydroxymethylformate and/or HCOOH+CH₂O, respectively. These two concerted paths are more or less equally demanding but the corresponding barriers (55.9 and 60.5 kcal mol⁻¹, respectively) are considerably higher than the barriers to the rearrangement and the decomposition of **B6**. If we now take into account that the barrier to the formation of **B6** from SOZ is unlikely to be very high, it is possible to conclude that, contrary to Dewar's claims,²⁸ the non-concerted path of SOZ decomposition *via* **B6** is quite probably more favorable than the concerted one.



Scheme 7. The values in parentheses (kcal mol⁻¹) refer to the activation barriers of individual reaction steps.

CONCLUSIONS

A comprehensive theoretical analysis of the gas-phase ozonolysis of ethene is presented using the semi-empirical quantum chemical method. This method allows consideration of all important reaction channels observed in the gas phase, and accounts for the observation of products such as oxiranes, OH radicals (possibly *via* hydroperoxycarbene (**M14**) or hydroperoxy acetaldehyde

(M13)). The method reveals some possible reaction channels that were not considered before. Even though the *absolute* accuracy of the calculations is less than that of some *ab-initio* methods, experience shows that the *relative* values of the different barriers are correctly predicted.

Acknowledgments. – This work was supported by the grant No. HRN-554-G-00-2078-00, US-Israel Cooperative Research Program, Human Capacity Development, Bureau for Global Programs, Field Support and Research USAID. The Farkas Center for Light Induced Processes is supported by Minerva GmbH, Munich.

REFERENCES

1. C. P. Schonbein, *J. Pract. Chem.* **66** (1855) 282.
2. P. Bailey, *Chem. Rev.* **58** (1958) 925–1010.
3. R. Criegee, in: *Houben Weyl Methods der Organische Chemie*, Stuttgart, 1952.
4. A. T. Menjailo and M. V. Pospelov, *Usp. Khim.* **36** (1967) 662–685.
5. A. Padwa, *1,3-Dipolar Addition Chemistry*, J. Wiley, New York, 1984.
6. P. Bailey, *Ozonation in Organic Chemistry*, Vol 2, Academic Press, 1978.
7. R. Atkinson, *Atm. Environ.* **24A** (1990) 1–42.
8. A. P. Altshuller, *J. Atm. Environ.* **17** (1983) 2383–2427.
9. R. Atkinson, *Chem. Rev.* **86** (1986) 69–201.
10. D. Grosjean, *Environ. Sci. Technol.* **24** (1990) 1428–1432.
11. R. Atkinson and A. C. Lloyd, *J. Phys. Chem. Ref. Data* **13** (1984) 315–444.
12. S. Gäb, E. Hellpointner, W. V. Turner, and K. Korte, *Nature* **316** (1985) 535–536.
13. K. H. Becker, J. Bechara, and K. J. Brockmann, *Atm. Environ.* **27A** (1993) 57–61.
14. N. M. Donahue, J. H. Kroll, J. G. Anderson, and K. L. Demerjian, *Geophys Res. Lett.* **25** (1998) 59–62.
15. R. Atkinson and W. P. L. Carter, *Chem. Rev.* **84** (1984) 437–470.
16. R. I. Martinez and J. F. Herron, *J. Phys. Chem.* **91** (1987) 946–953.
17. R. Atkinson, E. C. Tuazon, and S. M. Aschmann, *Environ. Sci. Technol.* **29** (1995) 1860–1866.
18. P. S. Nangia and S. W. Benson, *J. Chem. Soc.* **102** (1980) 3105–3115.
19. R. I. Martinez and J. T. Herron, *J. Phys. Chem.* **92** (1988) 4644–4648.
20. R. I. Martinez, J. T. Herron, and R. E. Huie, *J. Am. Chem. Soc.* **103** (1981) 3807–3820.
21. R. I. Martinez and J. T. Herron, *J. Phys. Chem.* **91** (1987) 946–953.
22. H. Kuhne, S. Vacani, A. Bander, and H. H. Grunthard, *Chem. Phys.* **28** (1978) 11–29.
23. F. L. Lovas and R. D. Suernam, *Chem. Phys. Lett.* **51** (1977) 453–456.
24. O. Horie, P. Neeb, and G. K. Moortgat, *Int. J. Chem. Kinet.* **26** (1994) 1075–1094.
25. O. Horie, P. Neeb, and G. K. Moortgat, *Int. J. Chem. Kinet.* **29** (1997) 461–468.
26. H. E. O’Neal and C. Blumstern, *Int. J. Chem. Kinet.* **5** (1973) 397–413.
27. R. Criegee, *Angew. Chem.* **87** (1975) 765–771.
28. M. J. S. Dewar, J. C. Hwang, and D. R. Kuhn, *J. Am. Chem. Soc.* **113** (1991) 735–741.
29. M. J. McKee and C. Mc Ralfing, *J. Am. Chem. Soc.* **111** (1989) 2497–2500.
30. L. B. Harding and W. A. Goddard III, *J. Am. Chem. Soc.* **100** (1978) 7180–7188.
31. D. Cremer, *J. Am. Chem. Soc.* **103** (1981) 3627–3633.

32. P. Hiberty, *J. Am. Chem. Soc.* **98** (1976) 6088–6092.
33. D. Cremer, E. Kraka, M. L. McKee, and T. P. Radhakrishnan, *Chem. Phys. Lett.* **187** (1991) 491–493.
34. R. Ponec, G. Yuzhakov, Y. Haas, and U. Samuni, *J. Org. Chem.* **62** (1997) 2751–2762.
35. M. Olzman, E. Kraka, D. Cremer, R. Guldbrod, and S. Anderson, *J. Phys. Chem A.* **101** (1997) 9421–9429.
36. D. Cremer, J. Gauss, E. Kraka, J. F. Hanton, and R. J. Bartlett, *Chem. Phys. Lett.* **209** (1993) 547–556.
37. R. Gutbrod, E. Kraka, R. N. Schindler, and D. Cremer, *J. Am. Chem. Soc.* **119** (1997) 7330–7342.
38. J. M. Anglada, J. M. Bofill, S. Olivella, and A. Sole, *J. Am. Chem. Soc.* **118** (1996) 4636–4647.
39. R. Gutbrod, R. N. Schindler, E. Kraka, and D. Cremer, *Chem. Phys. Lett.* **252** (1996) 221–229.
40. A. A. Granovsky, PC-Gamess can be downloaded on the address: <http://classic.chem.msu.su/gran/gamess/intex.html>
41. M. W. Schmidt, K. K. Baldrige, J. A. Boatz, S. T. Elbert, M. S. Gordon, J. J. Jensen, S. Koseki, M. Matsunaga, K. A. Nguyen, S. Su, T. L. Windus, M. Dupuis, and J. A. Montgomery, *J. Comp. Chem.* **14** (1993) 1347–1363.
42. R. W. Murray, *Accounts Chem. Res.* **1** (1968) 313–320.
43. H. Staudinger, *Chem. Ber.* **58** (1925) 1088–1096.
44. J. Z. Gillies, C. W. Gillies, R. D. Suenram, and F. J. Lovas, *J. Am. Chem. Soc.* **110** (1988) 7991–7999.
45. P. Bailey and A. G. Lane, *J. Am. Chem. Soc.* **89** (1967) 4473–4479.
46. D. P. Bartlett and M. Stiles, *J. Am. Chem. Soc.* **77** (1955) 2806–2814.
47. P. S. Mangia and S. W. Benson, *J. Am. Chem. Soc.* **102** (1980) 3105–3115.
48. R. Fajgar, J. Vitek, Y. Haas, and J. Pola, *J. Chem. Soc., Perkin Trans. 2* (1999) 239–248.

SAŽETAK

Teorijsko istraživanje mehanizma reakcije etana s ozonom i popratnih procesa u plinskoj fazi

Robert Ponec, Jana Roithova i Yehuda Haas

Prikazana je teorijska analiza reakcije etana s ozonom u plinskoj fazi. Potpuno pretraživanje kanala niskih energija otkrilo je nekoliko novih intermedijara i pružilo objašnjenje za učinkovito nastajanje radikala $\cdot\text{OH}$ pri ozonolizi etana u plinskoj fazi.